63-3-2

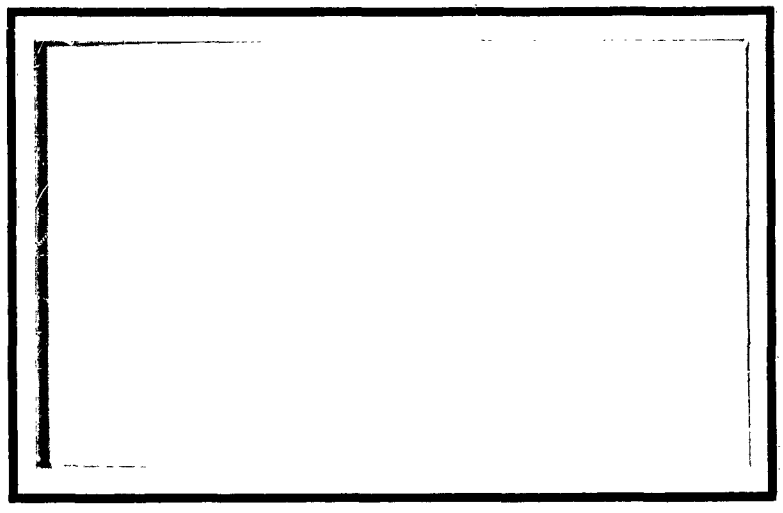

MICROWAVE DEVICES LABORATORY
DEPARTMENT OF ELECTRICAL ENGINEERING
UNIVERSITY OF UTAH
SALT LAKE CITY, UTAH

Research Sponsored by Contracts or Grants
U. S. Navy ONR Contract Nonr 1288(05)
National Science Foundation G-15017
Air Force Space Systems Division
Contract AF 04(647)-745
Air Force Aeronautical Systems Division
Contract AF 33(657)-8677

Microwave Devices Laboratory
Consolidated Quarterly Report
For the Period
October 1, 1962 to December 31, 1962

Technical Report MDL-Q3

December 31, 1962

Microwave Devices Laboratory
Electrical Engineering Department
University of Utah
Salt Lake City, Utah

TABLE OF CONTENTS

INTRODUCTION

The broad purpose of the research activity reported herein is to extend the useful frequency spectrum into the range from microwave frequencies to optical frequencies, and to improve existing devices and techniques in the microwave spectrum.

At present this objective is being pursued by studies of electron beam devices, solid state devices, and plasmas.

I. ELECTRON BEAM STUDIES

A. A 30-40 kMc Multiple-Ladder Circuit Backward-Wave Oscillator

Contract AF 33(657)-8677

L. S. Bowman, D. R. Gunderson, and R. W. Grow

The objective of this project is to investigate the feasibility of using multiple coupled ladders in backward wave oscillators at millimeter wavelengths. A 30-40 kMc oscillator is being constructed as a first step in this evaluation.

During this period the problem of a vacuum seal in the output waveguide was considered. No commercially available window was found that satisfied the requirements of 450° C bake-out temperature, stability in a vacuum, and low VSWR over a fairly wide frequency band. Investigation was performed into the possibility of using a long piece of ceramic material tapered to fill the waveguide and then tapered out again. The ceramic-to-metal seal would be vacuum tight and would be circular to cut down on mechanical stresses during joining.

A rectangular-to-round-to-rectangular waveguide transition section was designed, built, and tested at X-band. The VSWR of the transition section alone was found to be below 1.20 from 8.5 to 11 kMc. No specially-designed piece of ceramic material was tried in the section due to the high cost of fabrication, but results with various pieces of scrap ceramic indicate that this method will give a suitable output window at 40 kMc.

Attention was also given to lens action on the electron beam of the ladders in a 5,000 gauss field. The lens effects of the leading edges of the ladder planes upon the impinging beam do not appear to be a problem in the present design.

The amount of heat generated when the electron beam strikes the ladder planes at the leading edge will not be excessive under pulsed operation. Calculations indicate that a front ladder rung 0.0025" wide is needed to conduct away the heat for a 0.8×10^{-4} duty cycle.

The cold circuit losses for four ladder planes were calculated to be 9.76 db per inch of tube length by the following procedure. The loss is given by

$$L = 8.686\ \alpha \text{ db/meter}$$

where α is given by Pierce[1]

$$\alpha = \frac{\omega}{2Q\,|v_g|} = \frac{k}{2Q\left|\frac{\partial k}{\partial \beta}\right|} \approx \frac{\pi}{2c}\ \frac{k/k_c}{2Q}\left|\frac{\Delta\beta/k_c}{\Delta k/k_c}\right|$$

Pierce estimates the Q of an array of fine half-wave parallel wires to be

$$Q = \frac{\sqrt{\mu/\epsilon}}{R_s}\ \frac{v}{c}$$

where the surface resistivity for molybdenum is $R_s = 0.0948$ ohms per square at 40 kMc.

Since energy may be stored in the fields of each of the axial

---

[1] J. R. Pierce, Traveling-Wave Tubes, D. Van Nostrand Co., Inc., Princeton, N. J., 1950, pp.95-96.

space harmonics the Q becomes[2]

$$Q = \frac{\sqrt{\mu/\epsilon}}{R_s} \sum_{n=-\infty}^{\infty}{}' \frac{v_n}{c} = \frac{\sqrt{\mu/\epsilon}}{R_s} \frac{k}{k_c} \sum_{n=-\infty}^{\infty}{}' \frac{1}{\beta_n/k_c}$$

$$= \frac{\sqrt{\mu/\epsilon}}{2R_s} \frac{k}{k_c} \frac{p}{2c} \sum_{n=-\infty}^{\infty} \frac{1}{n + \frac{1}{2}\frac{\beta_o}{k_c}\frac{p}{2c}}$$

$$= \frac{\sqrt{\mu/\epsilon}}{R_s} \frac{k}{k_c} \frac{p}{2c} \frac{\pi}{2} \cot\left(\frac{\pi}{2}\frac{\beta_o}{k_c}\frac{p}{2c}\right)$$

Using the propagation curves and the design parameters we find $\frac{p}{2c} = 0.20$, $\frac{k}{k_c} = 1.93$, $\frac{\beta_o}{k_c} = 2.77$, $2c = 0.285$ inches, $\left|\frac{\Delta\beta/k_c}{\Delta\beta/k_c}\right| = 12.87$, $R_s = 0.0948$ ohms, $\frac{\pi}{2c}\frac{k/k_c}{2Q} = \frac{0.0948}{120\pi}\frac{5}{0.285}\tan 49.9° = 0.00525$ and the loss at the surface of a one ladder plane is

$$L = 8.686 \times 0.00525 \times 12.87 = 0.585 \text{ db/inch.}$$

Since the rungs and the slots are equal in width, the total surface current flows in only one-half of the total ladder plane length. Therefore, the actual current in the rungs is twice that allowed above so that the I^2R losses are four times as high, L = 2.34 db/in. (surface).

There remains the effect of ladder thickness, t = 0.005 inch. Per inch

---

[2] L. B. W. Jolley, Summation of Series, Second Revised Edition, Dover Publications, Inc., New York, 1961, p. 145.

of tube length, the slot side surface is

$$\frac{\lambda}{2} \times \frac{2t}{p} = \frac{\lambda}{2} \times \frac{0.010}{0.058} = 0.1723 \frac{\lambda}{2}$$

Since the loss for half-wave wires is 0.585 db/inch,

$$L_{side} = 0.1723 \times 0.585 = 0.10 \text{ db/inch}$$

and for four ladder planes,

$$L_{total} = 4(2.34 + 0.10) = 9.76 \text{ db/inch}$$

The design of the ladder structure was made by using this value.

Construction of the 40 kMc ladder circuit will begin immediately. Cold tests will next be made to optimize the design by experimental means.

B. Dielectric Slow-Wave Circuits
Contract Nonr-1288(05)
C. H. Durney and R. W. Grow

The objective of this project is to investigate the possibility of using small slow-wave circuits at millimeter wavelengths.

To verify experimentally the theory of the traveling-wave tube using a dielectric slow-wave circuit[3], an X-band traveling-wave tube using the circuit and electron beam configuration in Fig. 1 is being designed and constructed.

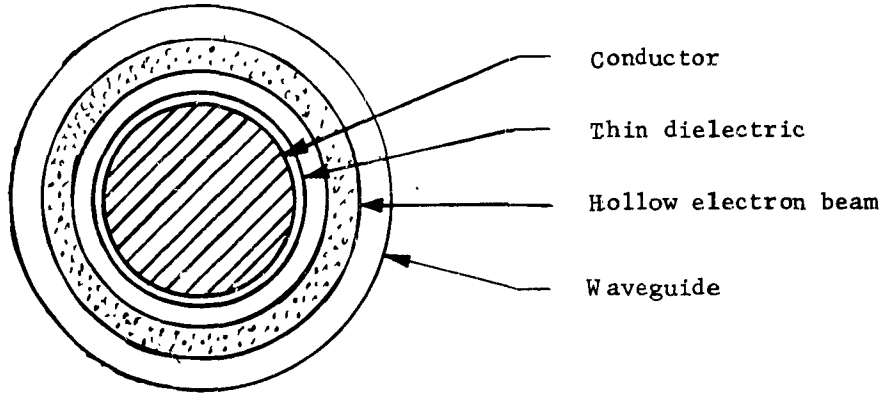

Fig. 1. Traveling-Wave Tube Circuit and Electron Beam.

The specifications of the tube for a gain of 18 db are as follows:

Dielectric tube

Inside diameter	1.3"
Wall thickness	.035"

[3] Report MDL-Q1, June 30, 1962, Microwave Devices Laboratory, University of Utah.

Length	8.0"
Relative dielectric constant	85
Electron beam	
Voltage (pulsed)	20,000 v.
Current density	2 amps/cm^2
Inside diameter	1.390"
Thickness	.050"
Separation from dielectric	.010"

Titanium dioxide has been selected for the above design. The titanium dioxide ceramic tubes will be obtained from an outside source.

The design of an electron gun which will produce the required hollow beam is nearly completed. It is hoped that it can be constructed and tested in the near future.

C. The Orbitron Amplifier
Contract AF 33(657)-8677
W. L. Dickson, R. L. Schriever, and C. C. Johnson

The objective of this project is to develop a high-efficiency, high-power amplifier utilizing the interaction between a spiraling electron beam and the fields in an unloaded waveguide.

During this period, additional work was done on the beam injection problem discussed in previous reports. Investigation of waveguide windows continued and the cold circuit for the device was designed.

Theoretically, a satisfactory injection scheme has been developed. It consists of a magnetron injection gun which produces a hollow rotating

beam of a certain radius in a magnetic field that is lower than the field required in the device. There is also a radial electric field present in the gun region. The rotating beam produced by the gun is passed into an electric field-free region where the radii of the individual electrons abruptly decreases. The beam is then accelerated axially, which stretches out the pitch of the electron trajectories. The magnetic field is then increased to the value required by the device. This field increase results in a decrease in the pitch angle of the individual electron trajectories and at the same time reduces the radii of the individual electrons and the radius of the entire beam so that the beam will fit into the waveguide.

The gun had to be designed so that the beam produced would, after passing through the field variations described above, result in a final beam that was satisfactory for use in the device. The design procedure is rather complicated and a good deal of time was spent in obtaining a suitable design. Such a design was accomplished and steps were made to secure data and electrode shapes from W. Waters so that the gun could be constructed.

A cold circuit was designed and fabrication was initiated. Since the interaction region in this device consists of a section of rectangular waveguide, it seems that fabrication of the circuitry would involve joining various bends, straight sections, and other shapes of waveguide stock to form the required circuitry; however, a much more satisfactory method of fabrication has been developed. In this scheme, a slot .4 inches wide and .9 inches deep is milled into a solid block of metal (aluminum for the cold circuit, copper for the actual tube). The slot is then covered with a piece of metal (the same metal as the

block into which the slot is cut). The resulting enclosed space is of the same dimensions as regular rectangular X-band waveguide. It is a fairly easy matter to make the slot conform to any preset pattern; consequently, intricate bends, tapers, slopes, and other required shapes in waveguide circuitry can be fabricated utilizing a milling machine with much greater ease than the same shapes can be made by fitting together sections of regular waveguide. The waveguide circuitry made by milling has the further advantage that it is much more rigid than is regular waveguide.

During this period, additional scaling, design, and measurements were made on waveguide windows in order that this problem might be fully solved when actual construction of the device begins.

During the next period, it is planned to test the cold circuit mentioned above. If the tests show that this circuit is satisfactory, then the circuit to be used in the device will be constructed. Also it is planned that the equations of motion of the electrons be analyzed on an analog computer. More detailed information on efficiency and gain is needed. Also, of particular importance, is the effect of pitch variation on tube performance. Construction of the electron gun will begin during the next period.

D. A Cyclotron-Synchronous Wave Amplifier
Contract Nonr-1288(05)
J. E. Dalley and C. C. Johnson

The objective of this experiment is to show that high efficiency can be obtained by employing an axially symmetric d-c pump structure to produce gain by coupling the fast cyclotron electron beam wave to the slow synchronous beam wave. With such an arrangement, the spent beam will be nearly mono-energetic, and it should be possible to depress the collector potential and obtain high efficiency.

Several modifications for the amplifier tube were suggested in the MDL-Q2 report. These modifications were made and the tube was re-assembled.

Gain was again achieved at low driving power using a magnetically shielded cathode. As the driving power was increased, the gain decreased without current interception in the pump or output coupler. This observation has not been satisfactorily explained yet.

The electron gun was placed in the full magnetic field in an attempt to obtain confined flow. Since the gun was designed for convergent brillouin type flow, the anode intercepted about 3/5 of the cathode current and the beam current was limited by anode dissipation. Sufficient beam current could not be obtained to load the cavities properly and gain could not be obtained. However, useful data were obtained on the collector design. It was found that the collector could be depressed to about 10 per cent of the beam voltage before serious reduction of beam current resulted.

A new tube is being designed which will use confined flow. An external cavity has been designed which will permit adjustments of frequency and coupling. It will be cold-tested soon, and if it is satisfactory, it will be incorporated in the new tube.

E. Multiple-Beam Interactions
Contract AF 33(657)-8677
P. J. Watts and R. W. Grow

The objective of this project is to investigate the possibility of using the interaction between multiple electron beams occupying the same space to build millimeter wave amplifiers and oscillators.

The investigation of the various modes of propagation on multiple electron beams is continuing. By taking d-c beam velocities in the z direction only and by assuming that the fields vary as $e^{j(\omega t + n\theta - \beta z)}$, a set of 3 second-order nonlinear differential equations have been written for multiple beam interaction.

$$\left[\gamma^2 r^2 - n^2 + k^2 r^2 \left(1 - \Sigma\, a_i \frac{\omega_i}{\omega}\right)\right] E_r + \left[jn\left(1 + r\frac{\partial}{\partial r}\right) - k^2 r^2 \Sigma\, j a_i \frac{\omega_c}{\omega}\right] E_\theta - \gamma r^2 \frac{\partial}{\partial r} E_z = 0,$$

$$\left[jn\left(1 - r\frac{\partial}{\partial r}\right) - k^2 r^2 \Sigma\, j a_i \frac{\omega_c}{\omega}\right] E_r + \left[\gamma^2 r^2 - 1 + r^2 \frac{\partial^2}{\partial r^2} + k^2 r^2 \left(1 + \Sigma\, a_i \frac{\omega_i}{\omega}\right)\right] E_\theta + jn\gamma r E_z = 0,$$

$$\left[\left(r + r^2 \frac{\partial}{\partial r}\right)\left(\gamma - \Sigma \frac{v_{oiz} a_i k^2 \omega_c}{\omega}\right) + \Sigma \frac{jn v_{oiz} a_i \omega_c k^2 r}{\omega_i \omega}\right] E_r + \left[jn\gamma r + k^2\left(r + r^2\frac{\partial}{\partial r}\right) \Sigma \frac{v_{oiz} a_i \omega_c}{\omega_i \omega} - \Sigma \frac{v_{oiz} n a_i k^2 r}{\omega}\right] E_\theta + \left[-r^2 \frac{\partial^2}{\partial r^2} - r\frac{\partial}{\partial r} - n^2 + k^2 r^2 \left(\Sigma \frac{\omega_{p_i}^2}{\omega_i^2} - 1\right)\right] E_z = 0$$

where

$$a_i = \frac{\omega_{p_i}^2}{\omega_c^2 - \omega_i^2}$$

$$j\omega_i = j\omega - \gamma v_{oiz}$$

ω_{p_i} = plasma frequency of the ith beam.

$$\omega_c = \eta B_{oz}$$

In this equation, all summations are taken over the number of beams and field quantities are assumed to vary as $e^{j(\omega t + n\theta - \beta z)}$ where $j\beta = \gamma$. Methods of simplifying and solving these equations are now being sought. Once the nature of the solution is known, the boundary conditions can be matched at the boundary of a finite beam and the propagation equations will result. It appears that a digital computer may be the only means for solving these equations for a specific example.

F. Magneto-Electric Beam Compression
NSF Grant 15017
L. Kikushima and C. C. Johnson

The objective of this study is to obtain a high current-density electron beam, of the order of 5,000 amperes per square centimeter, using magnetic compression in combination with a high convergence gun. A high perveance and high area compression electron gun designed by Frost, Purl, and Johnson[4] was selected for use in the magneto-electric

[4] R. D. Frost, O. T. Purl, and H. R. Johnson, "Electron Guns for Forming Solid Beams of High Perveance and High Convergence," Proc. I.R.E., Vol. 56, No. 8 (August, 1962) 1800-07.

compression system. Beam perveance and profile measurements were made on the new gun in a demountable beam tester. To make tests in a solenoid, a hard tube with an internal pole piece has been designed from the curves obtained in the computer study. A method to measure the beam diameter with the beam in a high magnetic field has been devised.

The problem of secondary emission from the collector of the demountable tester has been partially alleviated by coating it with carbon. Satisfactory perveance measurements were taken for the range of anode voltages from 500 volts to 10 kilovolts. The perveance measured was 2.4×10^{-6} which compares with the perveance of 2.2×10^{-6} reported for the original gun design.[4]

The 300 to 1 area convergence of the gun produces a beam which is so highly concentrated that beam profile measurements at 10 kilovolts are difficult to make. With the collector coated, profile measurements were taken at 2000 and 3000 volts. For beam voltages of 4000 volts and greater, the high density of the beam burned the carbon from the collector and made it impossible to get accurate measurements. Although the beam profiles were obtained at low voltages, they indicate that the gun has good characteristics and will be suitable for the tests to be made in a magnetic field.

In order to measure the beam diameter in a magnetic focusing field, a series of metal foil discs of various thicknesses will be stacked in front of the gun and the beam will be allowed to burn a hole through each one. By measuring the hole diameters as a function of disc thickness, it is hoped that a good estimate of the beam diameter and

current density profile will be obtained.

Future plans are to measure the magnetic field build-up through the pole piece that has been designed to see if the field has the desired axial variation and make any necessary changes in the shape of the pole piece. The gun will then be placed in the hard tube and tests made in a magnetic field.

II. SOLID STATE STUDIES

A. Irradiated Laser Materials

NSF Grant 15017
V. R. Johnson and R. W. Grow

The objective of this quarter's work was to obtain sufficient data on a γ-damaged ruby laser rod to verify the predictions of the last quarterly report (MDL-Q2). This has not been accomplished to date. The proper equipment for cleaning and resilvering the end planes of the ruby rod has been assembled. The resilvering was done by evaporating silver on the ends of the rod and using a photosensitive device to measure the transmissivity of the partially silvered end. This effort appears to have been successful, but the rod has not been used in a laser configuration to date.

Consistent data have not been obtained to date because of the poor condition of the xenon flash tube being used. A new tube with higher power and voltage ratings has been ordered and should be in use in a few weeks. As soon as consistent laser operation is again achieved, the attempt will be made to gather data on the effect of γ-damage on the threshold of ruby rods used as laser crystals.

B. Tunneling Studies

Contract Nonr-1288(05)
M.D. Crawford and R.W. Grow

The objective of this project is the study of quantum mechanic tunneling through thin barriers with possible application to:

1. Stimulated emission of radiation.

2. Interaction with and/or modulation of electromagnetic radiation.

3. Electron emission into a vacuum for use as a low-noise cathode.

During the period covered by this report, a new and unique device has been reported by numerous sources. The GaAs forward biased diode has emitted monochromatic light in the 8500 A° region. The important characteristics of this device when operated in coherrent or noncoherent modes are tabulated below.

Noncoherent Radiation Diodes:

1. Radiation intensity is a linear function of the diode current.[5]
2. Current-voltage relationship of the diode is of the form $I = K \exp(qv/2kt)$.[5]
3. Diode voltage increases and radiation bandwidth decreases as diode temperature decreases.[5]
4. No upper limit on the diode modulation frequency has been found.[5]
5. The possibility exists that the diode may provide part of its required refrigeration.[5]
6. The frequency of the radiation is determined by the gap energy of the semiconductor material used[5] and may be changed by using different semiconductors.[6]

Coherent Radiation Diodes:

1. Threshold current densities required for coherent light output have been reduced as a result of research effort from 10^4 amp/cm^2 to 100 amp/cm^2 in about one month.[6]

---

[5] Keyes, R. J. and Quist, T. M., "Solid-State Research," Lincoln Laboratory M.I.T., 1962, No. 2, pp. 8-13.

[6] "Electrical Engineering," Vol. 82, No. 1. pg. 41. (Editorial note by Eleanor F. Peck and Samuel Walters.)

2. Efficiencies of 20 to 50 percent have been obtained at 10 to 25 mw output power levels in continuous operation.[6]

Investigation of available information on GaAs lasers has had the following conclusions:

1. GaAs laser diodes are markedly different than GaAs tunnel diodes. The laser diodes exhibit no negative resistance region to indicate electron tunneling.
2. Conduction in the laser diode takes place through electrons in the "fermi tail" of the N-doped region which surmount the junction barrier.
3. Laser diodes may be operated in either cw or pulsed modes at high efficiencies. The power levels are limited in either case by heat dissipated in the diode.
4. No reports have been observed to date of the modulation characteristics of the laser diode with coherent output. It is expected that no difficulty will be encountered with diode modulation.

C. Millimeter Wave Masers
NSF Grant 15017
J. C. Clark and R. W. Grow

The objective of this project is to investigate materials suitable for use in solid-state masers at millimeter wavelengths.

During the period of this report, the main activity has been a search of the literature with a view to classify the materials used. It is hoped that such a classification will help give insight to guide further research.

Basically, a three level solid-state maser requires a microwave pump source to produce an inverted population distribution in a paramagnetic salt. A primary requirement of this type of maser is that transistions be allowed between nonadjacent energy levels. This suggests a classification by methods used to allow nonadjacent energy levels. Three different methods have been reported in present systems:

1. Mixing the electronic spin states by a noncubic crystal field.[7]
2. A type proposed by Bleany[8] in which a rare earth ion is in a cubic crystalline field where a Γ_8 quartet lies lowest.
3. Mixing spin states by the large magnetic interaction between the nucleus and the paramagnetic electrons in rare earth ions.[9]

The first group includes ruby (Cr^{+++} in Al_2O_3), rutile (Cr_{+++} in T_iO_2), and emerald (Cr^{+++} in $Be_3Al_2Si_6O_{18}$) which have all given successful maser action. In this case the zero field splitting is important in determining

---

[7]Bloemberger, N., "Proposal for a New Type Solid State Maser." Phys. Rev. Vol. 104, No. 2, October 15, 1956, pp. 324-327.

[8]Bleany, B., "A New Class of Molecules for Bloemberger-Type Masers," Proc. Phys. Soc., Vol. 73, pp. 937-939, 1959.

[9]Sabisky, E. S., and Lewis, H. R., "Holmium Doped Calcium Floride as a Maser Material," Proc. I.R.E., Vol. 51, pp. 53-56, January 1963.

the pump and signal frequencies that may be used. The Zeeman effect is in general not linear with applied field, and the energy levels are not symmetric except for a particular crystal orientation. Symmetry of the Zeeman levels is a necessary condition for push-pull or double pump operation that can be used on a four-level system to obtain a more favorable pump-to-signal frequency ratio.

The Bleany-type materials have no zero field splitting, but the Zeeman effect is linear and the energy level spacings can be changed by changing the orientation of the crystal with respect to the magnetic field. The energy levels are all symmetric irrespective of the angle of the magnetic field. This makes them ideally suited for use in the push-pull pumping scheme for any direction of the magnetic field.

In the third group, if the lowest energy state is a doublet, the hyperfine spectrum is isotropic for an ion in a cubic field. In this case the paramagnetic material may be used as a powder. The powder offers several advantages over the single crystal in that they are easier to prepare, they can give a larger filling factor in possible slow-wave structures, and rather complicated slow-wave structures may be used because of flexibility of the powder. Most hyperfine energy level spacing are in the order of 100 Mc with a few materials with a spacing as high as a few kilomegacycles. This puts the upper limit of frequency possible at about this level.

Opitcal pumping of microwave masers provides another class of materials that gives promise of giving low noise maser action at very high frequencies and at elevated temperatures. The mechanism is basically the same as for

the microwave pumped three-level maser except that the optical excitation process is employed for obtaining the inverted distribution in the atomic population density. From a knowledge of the transition probabilities, it is possible to determine the excess population in an upper state, the effective spin temperatures and the pump power requirements of the maser. The optical pump source may be the output of a laser or for some materials possibly a noncoherent light source.

Further investigation will continue on both Bleany-type materials and materials suitable for optical pumping.

III. PLASMA STUDIES

A. Waves in Plasmas
NSF Grant 15017
P. O. Berrett and C. C. Johnson

The objective of this program is to study plasma wave propagation in waveguides or microwave circuits and the interaction of these waves with electron beams for use as millimeter wave signal generators. The associated problem of coupling r-f power from the beam-plasma region to a suitable antenna system is also being considered.

Investigation of beam-plasma growth mechanisms for millimeter wave frequency generation is continuing having followed these steps:

a. The general solution to the wave equation in cylindrical coordinates for a lossless plasma was obtained by a coupled mode theory.

b. The determinantal equation for the propagation constant β for several of the simpler conductor-plasma-dielectric arrangements have been found. (Two were mentioned in the last Quarterly report.)

c. A study is in progress of ways of handling a solution when the beam is introduced.

The study referred to as step (c) may be summarized by showing that growing waves may be analyzed by at least four approaches:

1. A boundary value problem is solved treating plasmas as dielectrics with tensor permittivities and beams as Lorentz transformed plasmas. The work of step (b) may be directed in this direction.

2. Birdsall and Whinnery[10] have determined the propagation factor vs. beam admittance for space-charge waves in an electron beam. Another approach is to take the point of view that the plasma between the beam and the wall serves only as a medium through which the wall admittance is transformed to the beam boundary.

3. The beam may be treated as a moving plasma whose space charge wave action interacts strongly with the stationary plasma wave action when the Doppler shifted plasma frequency of the beam is near the plasma frequency of the stationary plasma.[11] This is essentially the double stream amplifier problem with one stream standing still. In a finite geometry the effect of the walls is to reduce the plasma frequency, an effect usually accounted for by the so-called "reduction factor."

4. The Cerenkov radiation approach in which the plasma appears to the bunches in the electron beam to be a medium with a phase velocity less than the vel ity of the beam electrons. Kenyon[12] has investigated the beam-plasma-unbounded dielectric problem from this point of view to the end of developing a Cerenkov coupler. It is to be decided if this approach merits utilizing to analyze growth in a closed region, the coupling being accomplished at the end of this region.

---

[10] Birdsall, Charles K. and Whinnery, John R., "Waves in an Electron Stream with General Admittance Walls," J.A.P., Vol. 24, No. 3, March 1953, pp. 314-323.

[11] Finkenstein, David, "Dynamics of Plasmas," Physics Today, Vol. 15, No. 12, December 1962, pp. 43-

[12] Kenyon, Richard J., "Cerenkov Radiation from an Anisotropic Plasma," Technical Documentary Report ASD-TDR-62-643, Technical Note No. 4, Ultramicrowave Section, Electrical Engineering Research Laboratory, Engineering Experiment Station, University of Illinois.

During this report period the greater share of attention was given to the beam admittance approach. Birdsall and Whinnery's[10] charts are for θ independent modes and for flows constrained by a very strong axial magnetic field. As an example, consider a beam of radius b centered in a plasma-filled circular guide of undetermined radius a.

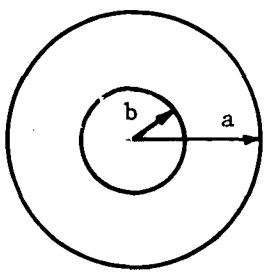

beam: $0 \leq r \leq b$

plasma: $b < r < a$

conductor: $r = a$

The problem is to determine the radius a at which the conducting cylinder is to be placed in order that the admittance presented to the beam at radius b be inductive, the condition necessary for growth. For the θ independent modes the pertinent fields in the plasma region of the guide are

$$E_z = A\gamma_1\xi \left[\frac{J_o(T_2a)}{J_o(T_1a)} \; J_o(T_1r) - J_o(T_2r) \right] e^{j(\omega t - \beta z)} \tag{1}$$

$$H_z = A\xi \left[-\frac{\gamma_1}{\gamma_2} \; \frac{J_o(T_2a)}{J_o(T_1a)} \; J_o(T_1r) + J_o(T_2r) \right] e^{j(\omega t - \beta z)} \tag{2}$$

$$H_\theta = \frac{\left[j\omega^3\mu_o(\epsilon_2^2 - \epsilon_1^2) + j\omega\beta^2\epsilon_1 \right] \frac{\partial E_z}{\partial r} + \beta\omega^2\mu_o\epsilon_2 \frac{\partial H_z}{\partial r}}{\left[\beta^2 - \omega\mu_o\epsilon_1 \right]^2 - \omega^4\mu_o^2\epsilon_2^2} \tag{3}$$

where

$$\epsilon_1 = \epsilon_o \left(1 - \frac{\omega_p^2}{\omega^2 - \omega_c^2}\right)$$

$$\epsilon_2 = \epsilon_o \left(\frac{-\frac{\omega_c}{\omega}\omega_p^2}{\omega^2 - \omega_c^2}\right)$$

$$\epsilon_3 = \epsilon_o \left(1 - \frac{\omega_p^2}{\omega^2}\right)$$

$$\gamma_{1,2} = \frac{(T_E^2 - T_H^2) \pm \sqrt{(T_H^2 - T_E^2)^2 + 4T_{EH}^2 T_{HE}^2}}{2 T_{HE}^2}$$

$$T_E^2 = \frac{\epsilon_3}{\epsilon_1}(\omega^2 \mu_o \epsilon_1 - \beta^2)$$

$$T_{HE}^2 = -j\omega \frac{\epsilon_2 \epsilon_3}{\epsilon_1} \beta \qquad \alpha = \omega\epsilon_1 - \frac{\beta^2}{\omega\mu_o}$$

$$T_H^2 = \frac{\omega\mu_o(\Delta\omega\mu_o + \beta^2\alpha)}{\omega\mu_o \alpha + \beta^2} \qquad \Delta = \left(\omega\epsilon_1 - \frac{\beta^2}{\omega\mu_o}\right)^2 - \omega^2\epsilon_2^2$$

$$T_{EH}^2 = \frac{j\omega^3 \epsilon_2 \beta \mu_o^2}{\omega\mu_o \alpha + \beta^2}$$

$$T_1^2 = T_E^2 - \gamma_1 T_{HE}^2$$

$$T_2^2 = T_E^2 - \gamma_2 T_{HE}^2$$

$$\xi = \frac{1}{\gamma_2 - \gamma_1}$$

We may then write the expression for admittance at a general radius $b < r < a$ as (for an E-type mode)

$$Y_E(r) = -\frac{H_\theta}{E_z}$$

$$= \frac{-\omega\left\{ j\left[\omega^2\mu_o(\epsilon_2^2 - \epsilon_1^2) + \beta^2\epsilon_1\right]\left[\frac{J_o(T_2a)}{J_o(T_1a)}\, T_1J_o'(T_1r) - T_2J_o'(T_2r)\right]\right.}{\left. + \beta\omega\mu_o\epsilon_2\left[-\frac{1}{Y_2}\,\frac{J_o(T_2a)}{J_o(T_1a)}\, T_1J_o'(T_1r) + \frac{T_2}{Y_1}\, J_o'(T_2r)\right]\right\}}{\left[\frac{J_o(T_2a)}{J_o(T_1a)}\, J_o(T_1r) - J_o(T_2r)\right]\left\{\left[\beta^2 - \omega^2\mu_o\epsilon_1\right]^2 - \omega^4\mu_o\epsilon_2^2\right\}} \qquad (4)$$

The steps to a solution are:

1. Decide what $\beta = \beta_{re} + j\,\beta_{im}$ is desired and realizable (from the consideration that in a lossless case the perfectly conducting wall can transform only to a pure susceptance).
2. Use Birdsall and Whinnery's curves to determine $Y_E(b)$.
3. Equate the required $Y_E(b)$ of (2) to $Y_E(r)$ of Eq. 4 evaluated at $r = b$. This is the transcendental equation yielding the radius a at which the conducting wall must be placed.

Emphasis will now be given to consolidating the survey to date and to decide upon the most promising avenue to the design of a tube. Particular attention is to be paid to cyclotron-wave coupling for possible use as a millimeter-wave device, and to the coupler problem.

B. Plasma Generation and Measurements
NSF Grant 15017
Verle Gilson and C. C. Johnson

The object of this project is to compare electron densities that have been determined by Langmuir double probes[13] with those determined by a microwave resonant cavity for a mercury arc discharge, to determine the accuracy of Klarfeld's predictions[14] of electron density and temperature for small diameter discharges, and to obtain electron density characteristics of a 1 cm. diameter mercury discharge in the presence of a static axial magnetic field.

In the last quarterly report, it was stated that data had been obtained from a 1.0 cm. diameter mercury discharge with and without an axial magnetic field applied; however, it was learned afterwards that the tube had a small air leak in one of the probes which had altered the discharge characteristics and rendered the data questionable. Since that time the tube has been repaired and new Langmuir double probe and resonant cavity data have been obtained for discharge currents ranging from 0 to 450 ma. at 50 ma. intervals, and for axial magnetic fields from 0 to 1000 gauss at selected intervals. All nonmagnetic field double probe and resonant cavity data have been interpreted to yield the electron temperature and density. The resonant cavity data for axial magnetic field conditions

---

[13] Johnson, E. O. and Malter, L., "A Floating Double Probe Method for Measurements in Gas Discharges," Phys. Rev., Vol. 50, p. 58, October (1950).

[14] Klarfeld, B., "Characteristics of the Positive Column of Gaseous Discharges," Journal of Phys. Acad. of Sci., USSR, Vol. 5, p. 155 (1941).

have been used to determine how the density is affected by magnetic field.

In the last quarterly report, an equation was derived which enabled the discharge ion density determined by double probes to be within reasonable agreement with the electron density determined by a resonant cavity for a 0.381 cm. diameter mercury discharge. The equation is

$$n = \frac{I}{eA_s} \left(\frac{M}{kT} \right)^{1/2}$$

where

I = ion saturation current

M = ion mass

k = Boltzman constant

T = electron temperature

e = 1.6×10^{-19} coulomb

A_s = surface area of the probe sheath determined by Langmuir's space charge equation

This same equation was used to determine the ion density plot of Fig. 2 for the 1.0 cm. discharge. The electron temperature T, determined from double probe data by Johnson and Malter's equivalent resistance method,[13] was found to be constant at 35,500° K for all values of discharge current, which agrees with Klarfeld's predicted value of approximately 36,000 degrees. In the same figure, densities determined by a cylindrical cavity 17.3 cm. long and 3.18 cm. radius are plotted along with Klarfeld's predictions so a comparison can be made. It is interesting to note that while the density determined by probe number 1 agrees quite well with the cavity density, probe number 2's density does not. It appears that the

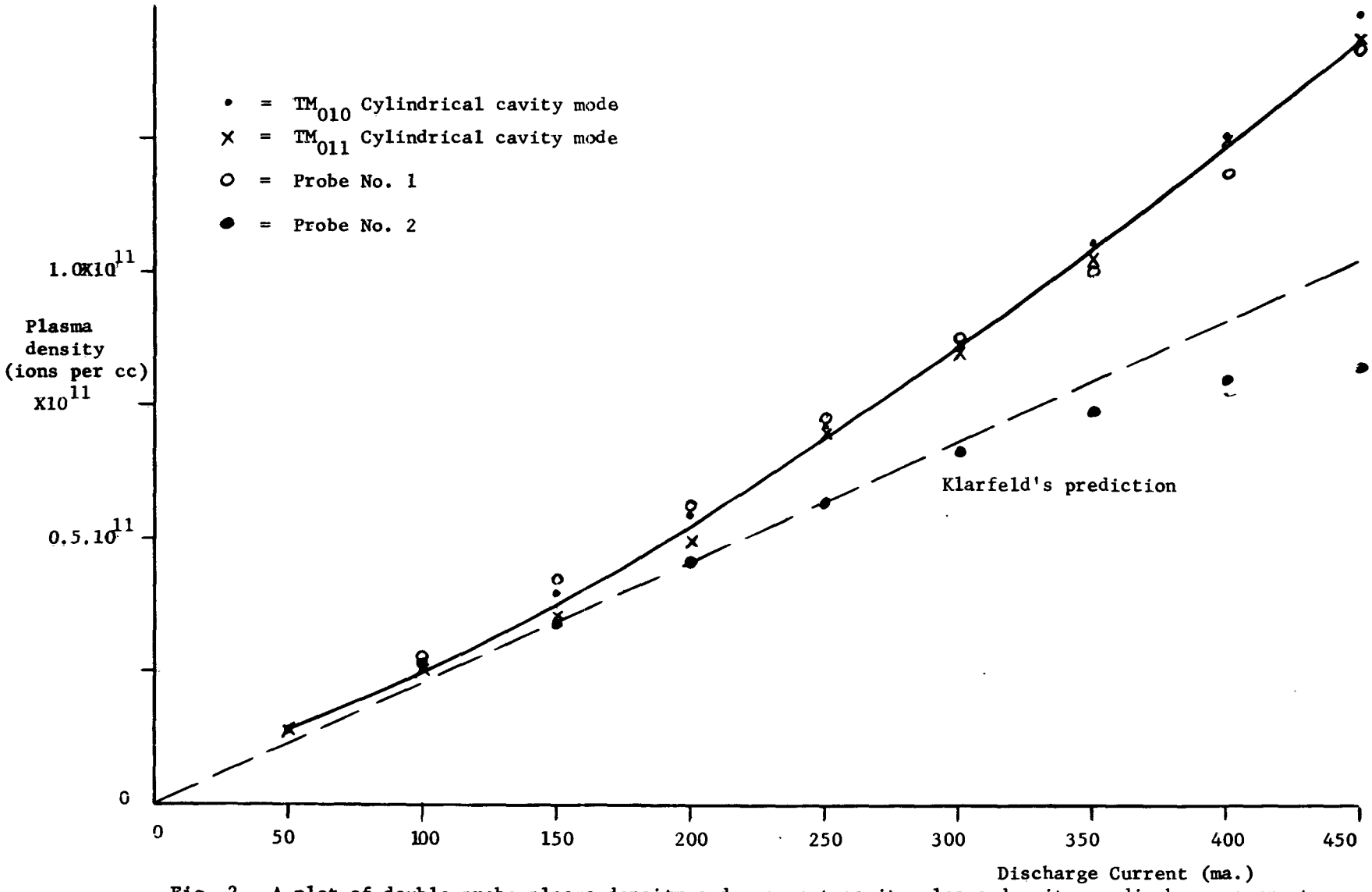

Fig. 2. A plot of double probe plasma density and resonant cavity plasma density vs. discharge current in a 1 cm Hg. discharge with zero magnetic field.

the number 1 probe may have shielded the number 2 probe from some of the ions causing the number 2 probe to predict a lower density. A more careful study will be made on this observation.

Figure 3 shows how the electron density, when determined by the resonant cavity, varied with magnetic field. It can be observed in the figure that the density increased as B was increased, to approximately 200 gauss, where saturation occurred. The average of the influence that the magnetic field had on the density is shown in Fig. 4. The region between 0 and 200 gauss is particularly interesting because it resembles an effect caused by a diffusion coefficient, normal to the applied field, that is a function of the field. The diffusion coefficient, according to Francis,[15] is

$$D = \frac{D_o}{1 + \omega^2/\nu^2} \tag{5}$$

where

D_o = diffusion coefficient with no B field

ω = electron cyclotron frequency

ν = electron collision frequency

Assuming that the average electron density in the plasma can be represented by the equation

$$n = \frac{A}{D} \tag{6}$$

---

[15] Francis, G., Handbuch Der Physik, Springer-Verlag, Berlin, V. 22, p. 169, (1956).

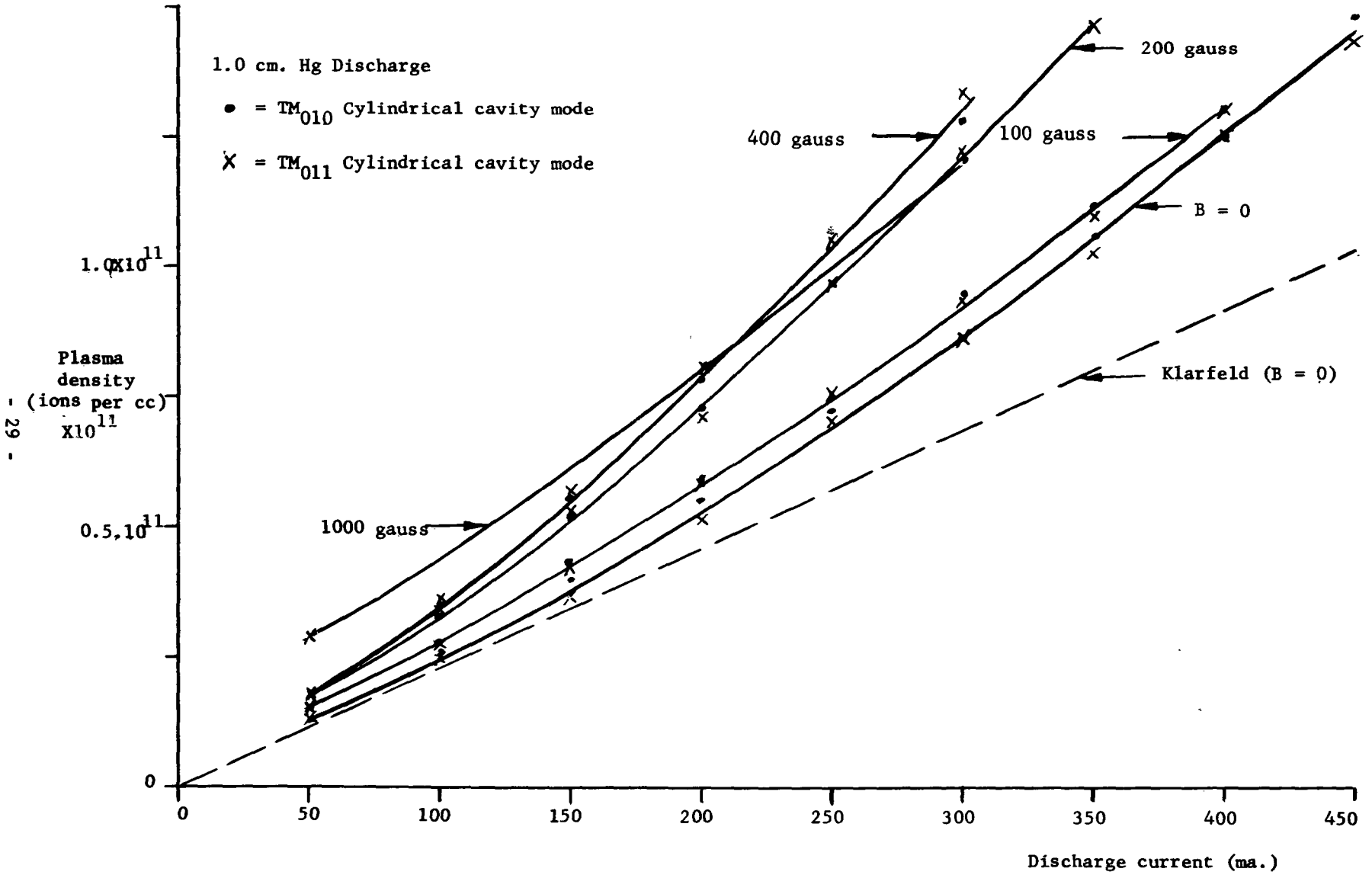

Fig. 3. A plot of plasma density vs discharge current and magnetic field for a 1.0 cm. mercury arc determined by a cylindrical microwave cavity.

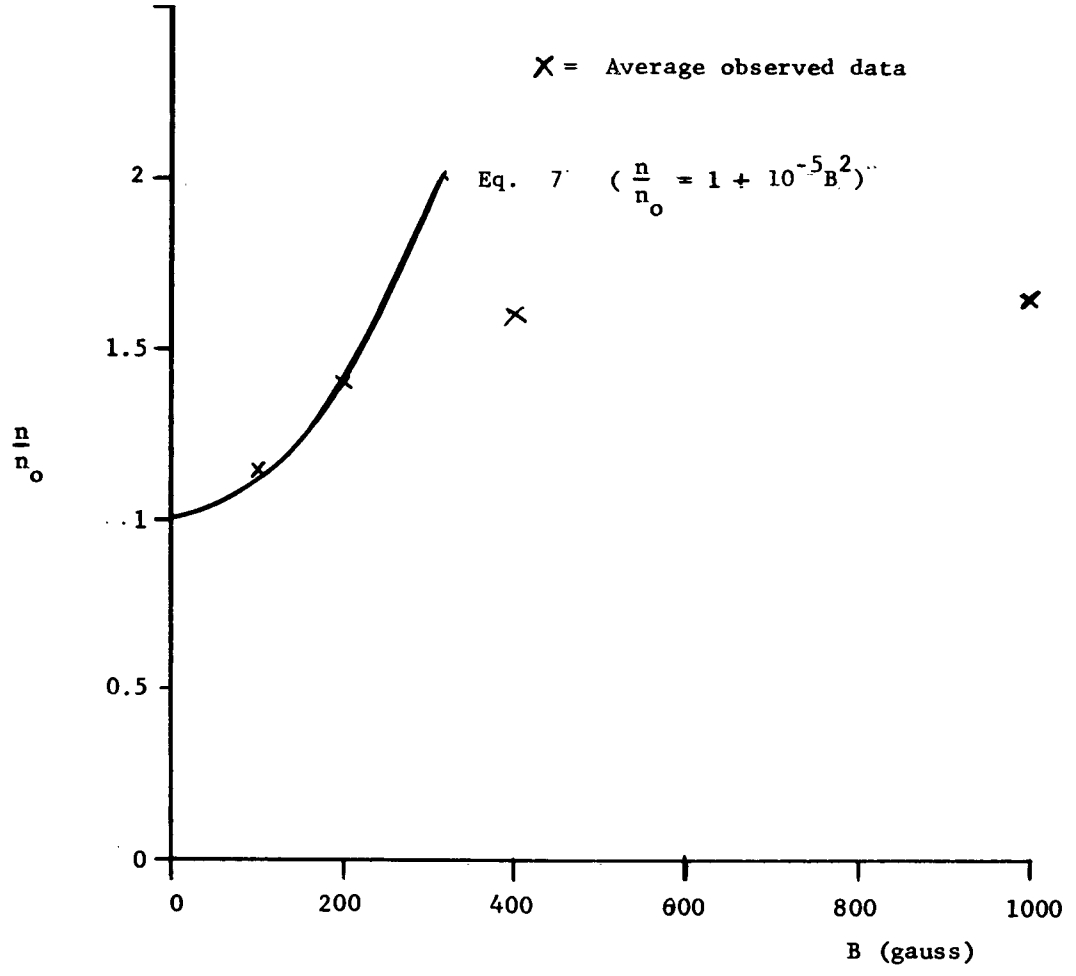

Fig. 4. A plot of the average influence of magnetic field on the electron density in a 1.0 cm. diameter mercury discharge and the curve $\frac{n}{n_o} = 1 + 10^{-5}B^2$ (Eq. 7.)

where

A = constant

D = diffusion coefficient

the expression for the density as a function of magnetic field, using Eq. 5, becomes

$$n = \frac{A(1 + CB^2)}{D_o} \tag{7}$$

where

B = magnetic field

$C = \left(\frac{e}{m\nu}\right)^2$

$\frac{e}{m} = 1.76 \times 10^{11}$ coul/kg.

Dividing both sides of Eq. 7 by the average electron density n_o for the case of no B field and taking the derivative with respect to B of both sides, the equation can be reduced to

$$\frac{A}{D_o n_o} = \frac{d\left(\frac{n}{n_o}\right)}{dB} \frac{1}{2C^2 B} \tag{8}$$

Using the average measured values of $\frac{n}{n_o}$ and B in Fig. 4, Eq. 8 reduces to the approximate value

$$\frac{A}{D_o n_o} \approx \frac{10^3}{C^2} \tag{9}$$

The difference between the density at some value of magnetic field and the density with no field is

$$n - n_o = A\left(\frac{1}{D} - \frac{1}{D_o}\right) \tag{10}$$

Using Eqs. 5 and 9, Eq. 10 reduces to

$$\frac{n}{n_o} = 1 + B^2 \times 10^{-5} \tag{11}$$

where B is in gauss. The above equation is also plotted in Fig. 4. In the preceding discussion, volume recombination in the plasma has been neglected; however, above 200 gauss it appears as if volume recombination began to show its influence and the electron density saturated at a level determined by volume recombination effects. Assuming the electron temperature remained constant at 35,000° K, the electron cyclotron radius, determined by solving for the electron velocity from the equation

$$v = \left(\frac{2kT}{m}\right)^{1/2}$$

where

$T = 35{,}500°$ K

m = electron mass

k = Boltzman constant

is

$$r_c = 0.3 \text{ mm.}$$

Since the radius of the tube is 5 mm, the cyclotron radius was 6/100

that of the tube. It is interesting to note that, assuming a uniform density in the discharge, the ratio of the total number of electrons that could not possible make it to the wall following a collision to the total number in the discharge was

$$R = (1 - \frac{r_c}{a})^2$$

$$= 0.885$$

where

$$r_c = 6/100\ a$$

It is assumed that the electron's maximum excursion in the radial direction as one cyclotron radius. Thus the density saturation, caused by volume recombination, apparently began to occur when the electron's mean free path in the radial direction was approximately 6 per cent of the tube radius which corresponds to 90 per cent of the electrons being unable to reach the wall following a collision. This is based on the assumptions that the electron temperature was independent of magnetic field strength and the discharge contained a uniform electron density.

In the future effort, we will compare the densities determined by double probes with the cavity densities while the magnetic field was applied, obtain a density vs. axial position profile by means of a short movable resonant cavity to justify comparing the double probe densities with the cavity densities, obtain density vs. mercury pool temperature and tube wall temperature vs. discharge current relationships, and attempt to observe any oscillations that may exist in the discharge. All of this work will be done on the 1.0 cm diameter mercury tube.

C. Microwave Plasma Measurements
NSF Grant 15017
J. C. Lee and C. C. Johnson

The object of this project is to investigate plasma waves experimentally for the purpose of verifying wave theory and providing a technique for measuring plasma parameters.

During this period a series of standing-wave measurements was made. A radio-frequency signal was introduced onto the discharge through an anode-coupler, and a standing-wave pattern was set up by reflected energy from the unterminated end of the plasma waveguide. Wavelengths were measured by a movable probe inserted in the slotted cylindrical waveguide. The temperature of the mercury pool was kept at 25°C.

Stray fields outside the cylindrical waveguide and inside the solenoid gave rise to extraneous modes. When lossy paper was inserted in the solenoid, these modes were suppressed. Very peculiar wave patterns near cut-off were observed. As the probe was moved from anode end to cathode end along the slot, the field strength was found to vary in an irregular fashion. Below cut-off, the distances between adjacent peaks and nulls were found fluctuating along the guide about some "average value." The ω-β diagrams for both $B \neq 0$ and $B = 0$ are plotted as shown in Figs. 5 and 6. The plasma frequencies, ω_p, were calculated from electron density data furnished by V. Gilson of this laboratory. It is seen from the curves that ω_p values from wave measurements are higher than those from probe and cavity measurements.

The modes of propagation considered here are electromechanical in nature in which the electron density within the plasma column or on its surface

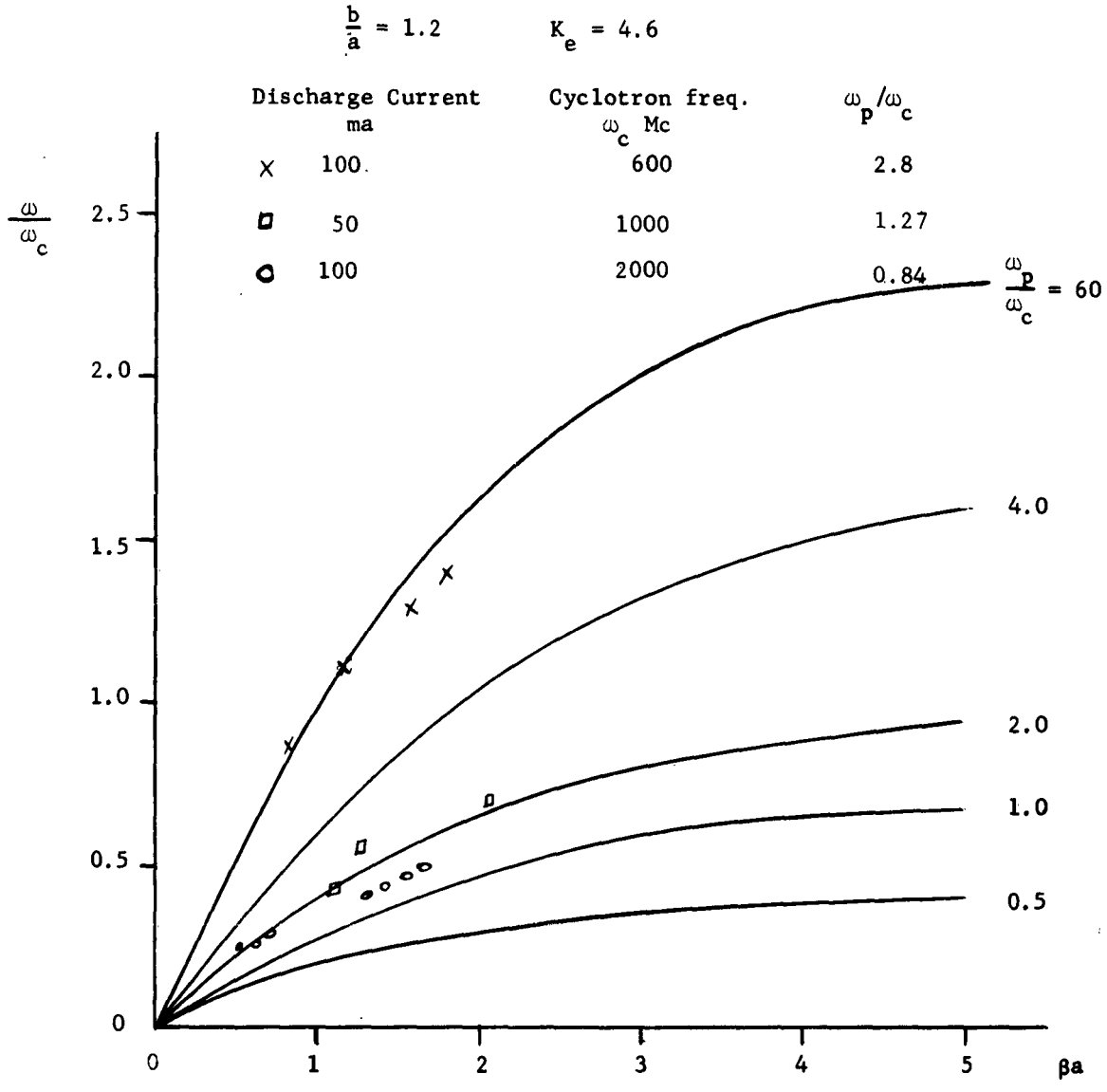

Fig. 5. ω-β diagram for space-charge waves for B ≠ 0

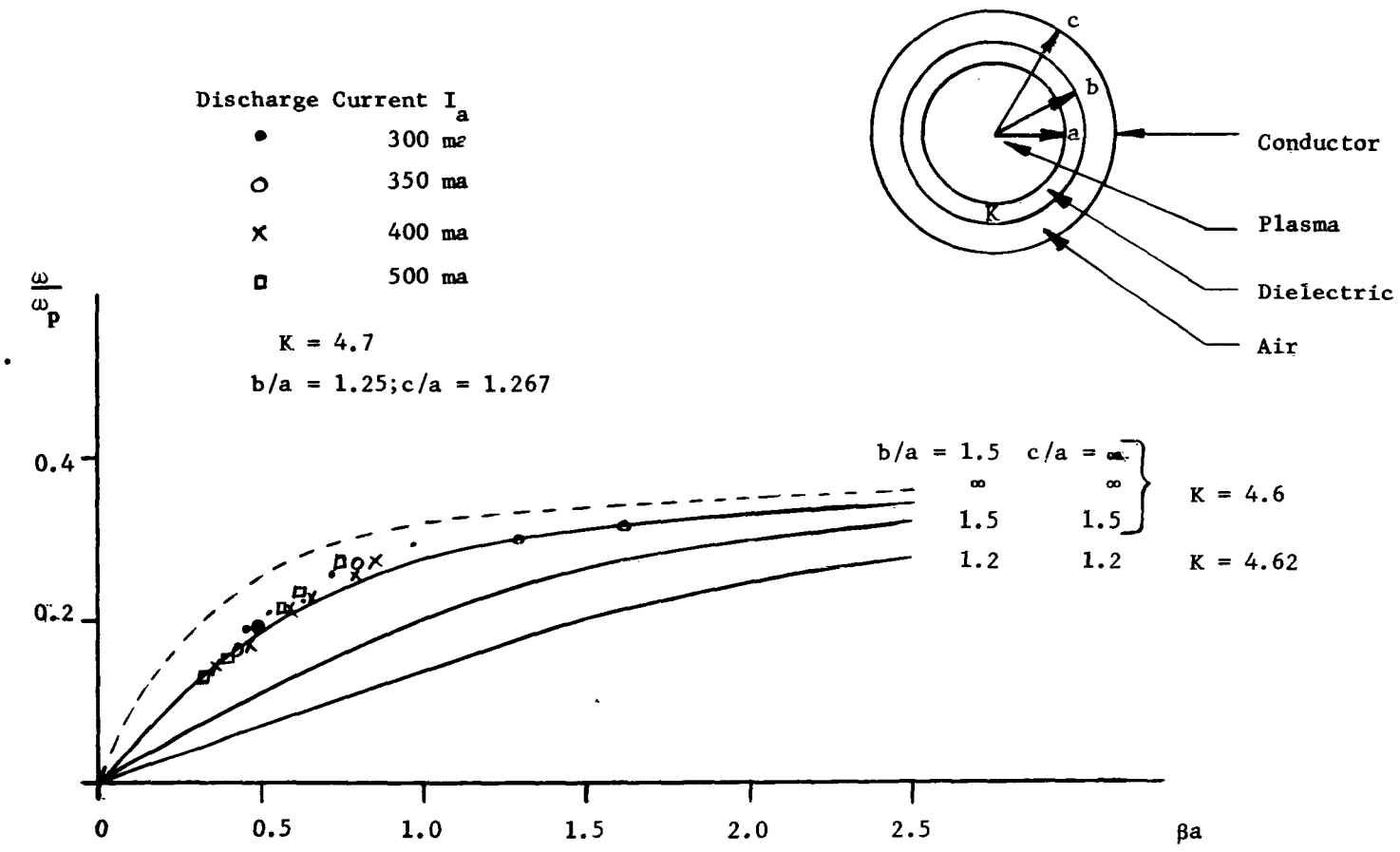

Fig. 6. ω-β diagram for surface waves (B = 0)

is modulated as the wave passes. These space-charge waves are quite different from the modes of the hollow circular waveguide perturbed by a plasma column; they can propagate below the waveguide cut-off. In the absence of a d-c magnetic field, the plasma guide modes are called surface waves. By using the large argument approximation for the Bessel functions, the cut-off frequency for surface waves is given by

$$\omega_{co} = \omega_p (1 + K)^{-1/2} \qquad (12)$$

where ω_p is the plasma frequency and K the dielectric constant. For very large values of βa, the field exists chiefly in the vicinity of the plasma-dielectric interface. An air region can exist between the dielectric and the metal cylinder without changing the relation of Eq. 12. Because of this indifference to geometry, the experimental data at cut-off should agree with the theoretical cut-off relation much closer. And this is true, as shown in Fig. 7, where the plasma frequencies were again calculated from the electron density data furnished by V. Gilson, and the cut-off frequencies were measured by varying the frequency of the signal generator and watching for the start of response shown on a standing wave indicator. As the surface wave dispersion curve approaches cut-off asymptotically, the reading should be fairly close to true cut-off. An interesting feature of this result is that it seems to be of value in plasma diagnostics. The measurement of cut-off surface waves discussed here may be developed to be a new and easy way of determining electron densities in a plasma.

For the next period, it is planned to investigate the use of the transverse probes to excite the backward-wave modes.

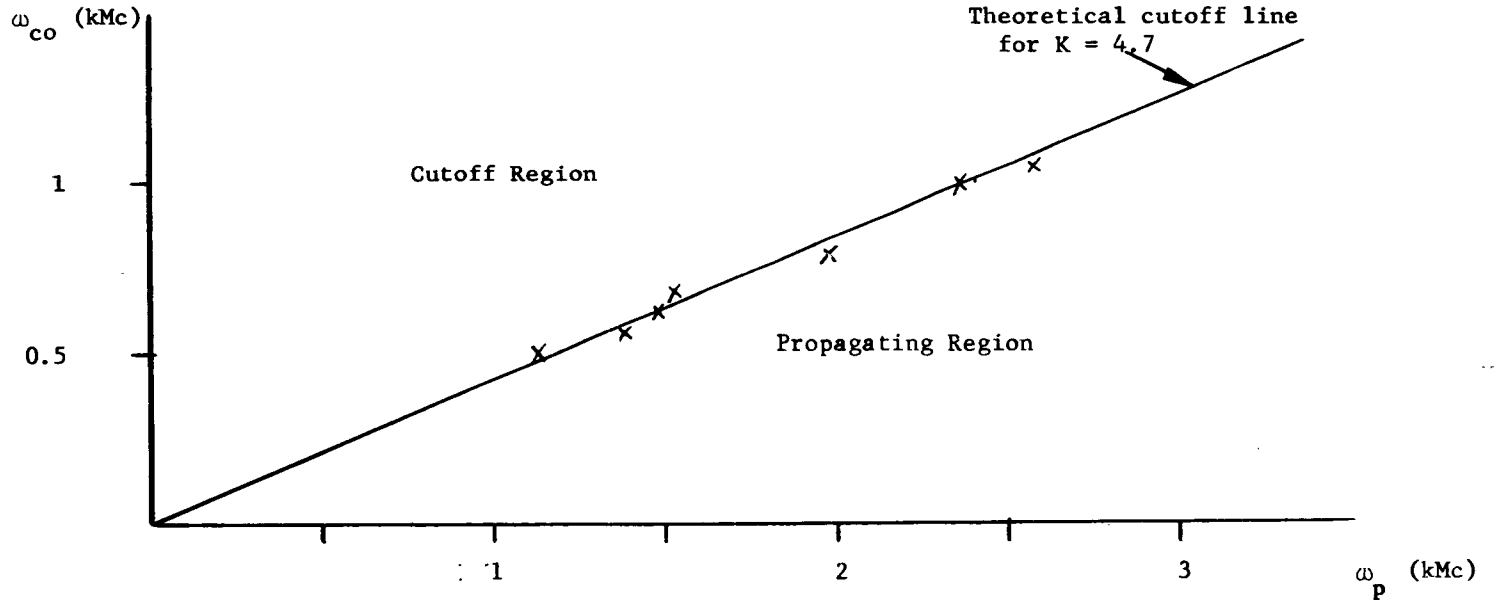

Fig. 7. Experimental data for cutoff relation for surface waves.

D. Rocket Exhaust Studies
Contract AF 04(647)-745
A. S. Jones, C. C. Johnson, and R. W. Grow

The purpose of this project is to establish theoretical and experimental techniques which enable the measurement of electron concentration in a plasma with microwave radiation. The plasma used in this project is the exhaust of a solid fuel rocket engine. The exhaust is a stratified mixture of ionized gases and particles.

During the past quarter, error analyses have been carried out to find the effect of using various values for the ratio of specific heats in the plasma and various values of the ionization potential. An investigation has been made on the increased information that can be obtained using additional frequencies. At wave frequencies much greater than either the plasma or collision frequencies of the medium, the variation of attenuation with frequency is given by

$$A = \frac{\text{constant}}{\omega^2} \tag{13}$$

When ω is so great that Eq. 13 is valid for a region where ω is bounded by ω_1 and ω_2, then an attenuation measurement at ω_1 and ω_2 is no better than an attenuation measurement at either frequency, inasmuch as the information gained at both frequencies will be simply the "constant" in Eq. 13. In order to determine if additional frequencies above our highest frequency, 23 kMc, will yield additional information, the exact attenuation equation was plotted as a function of frequency and is shown for one particular plasma in Fig. 8. For comparison an inverse square curve is also shown

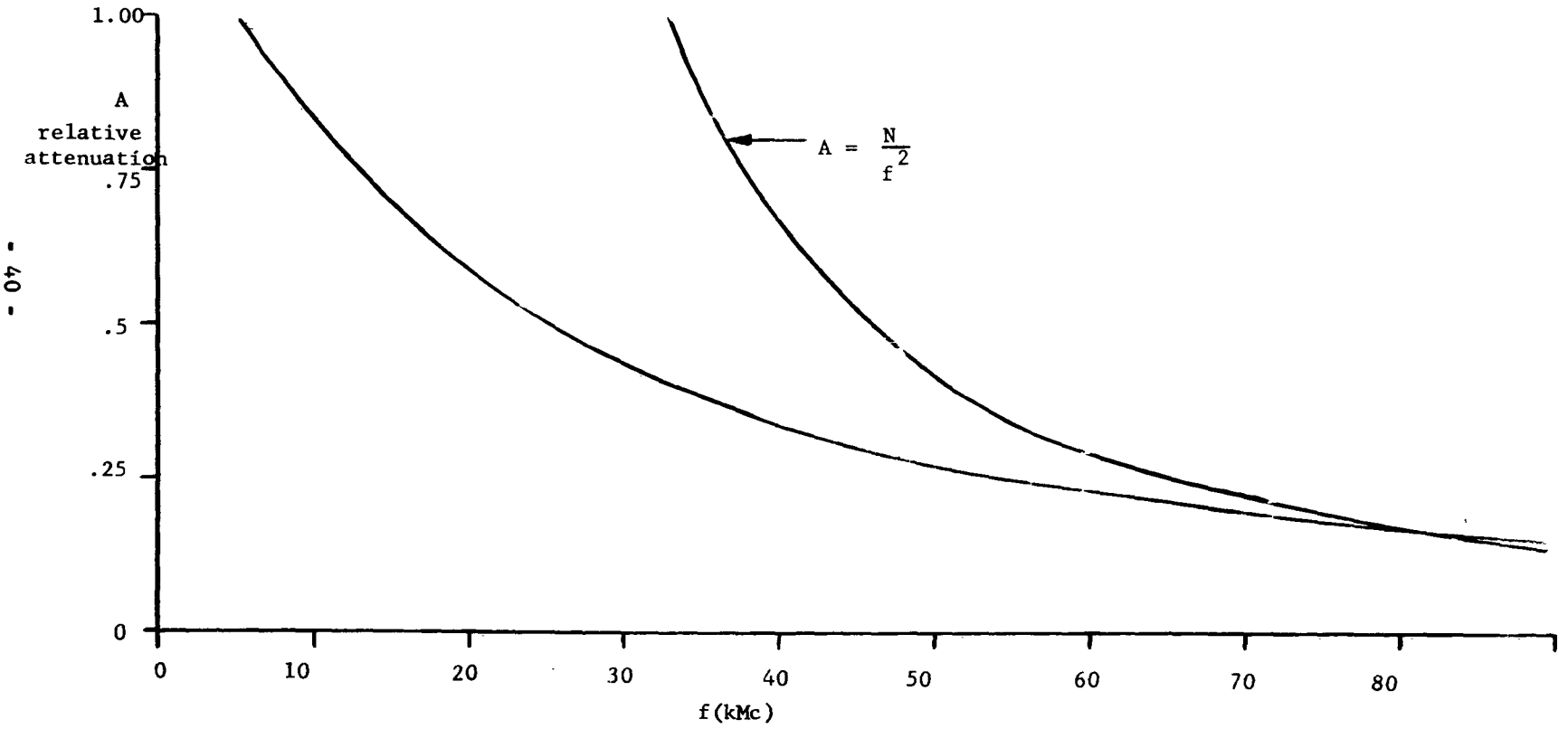

Fig. 8. Attenuation versus frequency

in Fig. 8. It is apparent that in the present case additional data can be obtained by using a third frequency at 60 kMc.

As the ratio of specific heats varies, the exit plane pressure and therefore the shockwave configuration varies. Figure 9 shows the relative

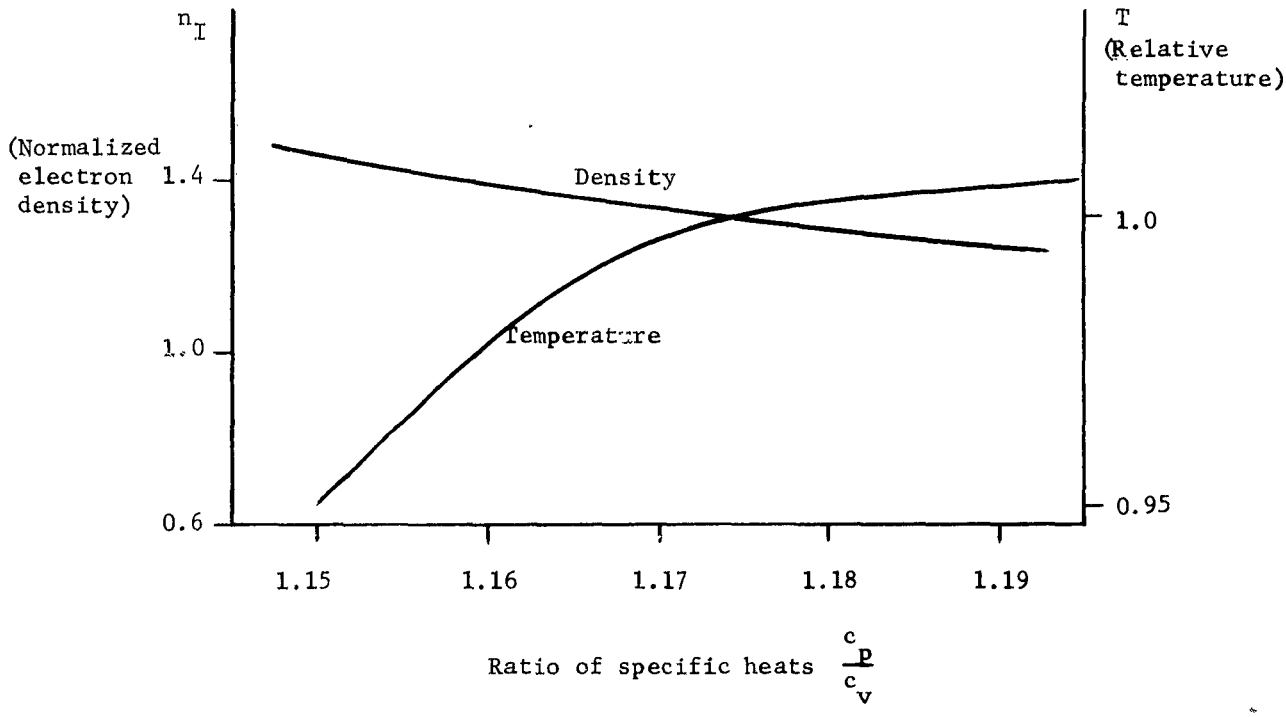

Fig. 9. Variation of electron density and temperature with the variation of the ratio of specific heats.

variation of temperature with the ratio of specific heats, and the relative variation of electron density with c_p/c_v.

Relative variation of electron density and temperature with ionization potential is shown in Fig. 10. It is hoped that this variation will provide a conclusive answer as to the source of electrons in the plasma.

In the next quarter, additional experimental data will be analyzed with greater experimental precision in order to determine the desired parameters more correctly. Additional work on the variation of parameters will be carried out.

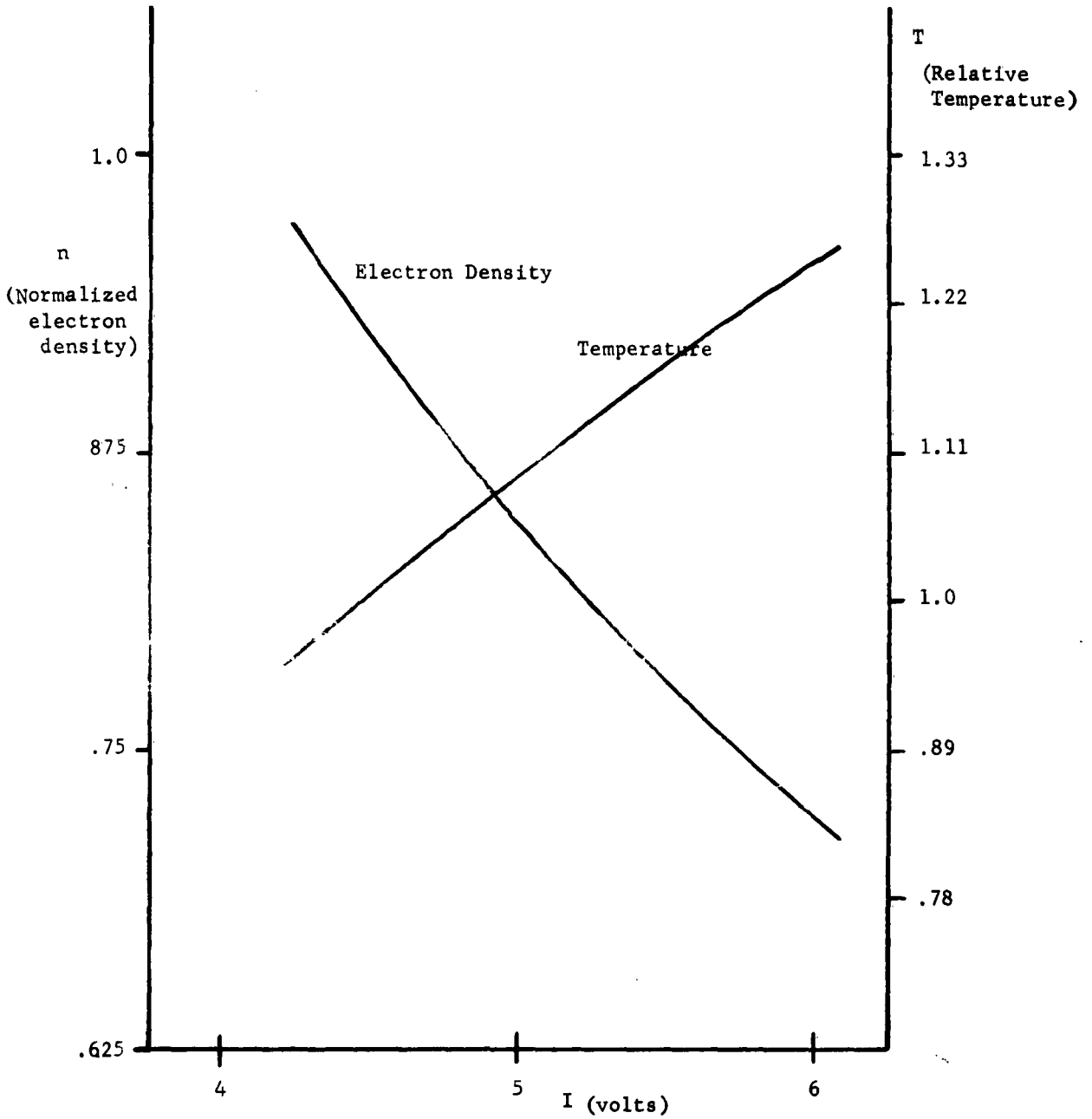

Fig.10. Variation of electron density and temperature with ionization potential.

E. Thermionic Emission from Condensed Species in Rocket Exhausts
Contract AF 04(647)-745
C. C. Johnson, A. S. Jones, and R. W. Grow

The objective of this study is to consider the nature of a thermionically emitting particle in a hot plasma. An electron cloud will be generated in the vicinity of the particle, and the interaction of this electron cloud with the plasma is to be considered.

It has been suggested by various workers[16,17] that thermionic emission from particles within a rocket exhaust plasma is a major contributor to the plasma electron density. A thermionically emitting particle in a plasma will generate a cloud of electrons in the immediate vicinity of the particle and will also contribute to the electron concentration in the plasma. Since the emitting characteristics of the particle are profoundly influenced by the space-charge cloud near the particle, it is necessary to carry out a space-charge analysis to accurately calculate the contribution to the plasma electron density from particle thermionic emission.

A planar analysis of the emission problem may be quite easily handled analytically. However, the particles in a plasma are of extremely small size and the characteristics are determined to a great extent by the spherical geometry of the particle. Therefore an accurate description for the emission phenomena requires a solution to Poisson's equation in spherical coordinates. Since there are no angular variations, Poisson's equation reduces to

$$\frac{d^2V}{dr^2} + \frac{2dV}{rdr} = - \frac{\rho}{\epsilon_o} \qquad (14)$$

---

16 Einbinder, H., "Generalized Equations for the Ionization of Solid Particles," Journal of Chem. Physics, 26, pp. 948-953, April 1957.

17 Smith, F., "On the Ionization of Solid Particles," Phys. Rev. Letters, p. 747-749, 1958.

where from Boltzman's equation

$$\rho = \sum_i eZ_i \rho_i \, e^{-\frac{eZ_i V}{kT}}$$

and

eZ_i = charge on i^{th} molecular species

ρ_i = i^{th} molecular species number density

A solution to this problem has been carried out in the Debye-Hückel theory for the case where $eZ_i V/kT \ll 1$. The results are

$$V = \frac{Q}{4\pi\epsilon_o r} e^{-kr}$$

where

$$k^2 = \frac{e^2}{\epsilon_o kT} \sum_i Z_i^2 \rho_i$$

Equation 14 was solved numerically on the IBM 1620 computer for electrons only. The print-out yields V and ρ as a function of r. Figure 11 shows the charge density distribution for a given set of parameters and it is noticed that the electron cloud density is very great near the particle surface and decreases very rapidly as r increases. It is noticed that the total voltage difference is on the order of one volt, thus the Debye-Hückel approximation is not valid. Figure 12 shows similar data where plasma electrons, positive ions, and negative ions are taken into account. This figure is for a given set of parameters where the plasma electron density is considerably greater than the electron density contribution due to thermionic emission.

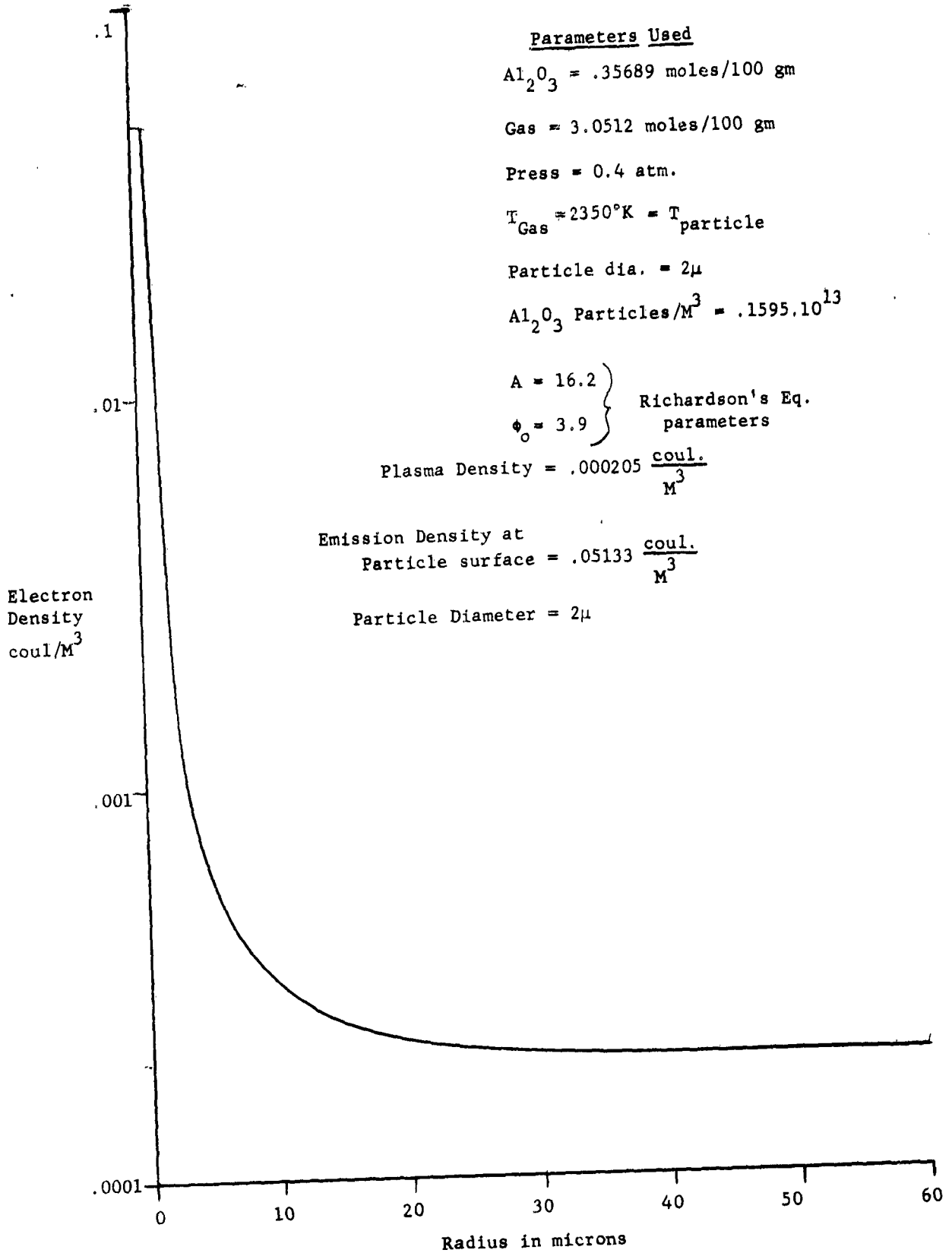

Fig. 11. The radial variation in electron density around an aluminum oxide particle is shown. The electron density falls off very rapidly away from the particle surface.

Al_2O_3 = .3568 moles/100 gm Positive Ions = .003 coul/M^3

Gas = 3.051 moles/100 gm Negative Ions = .033 coul/M^3

Press = .4 Atm. Plasma Electron = .030 coul/M^3

R(V'=0) = 25μ Thermionic Electron = .0002 coul/M^3

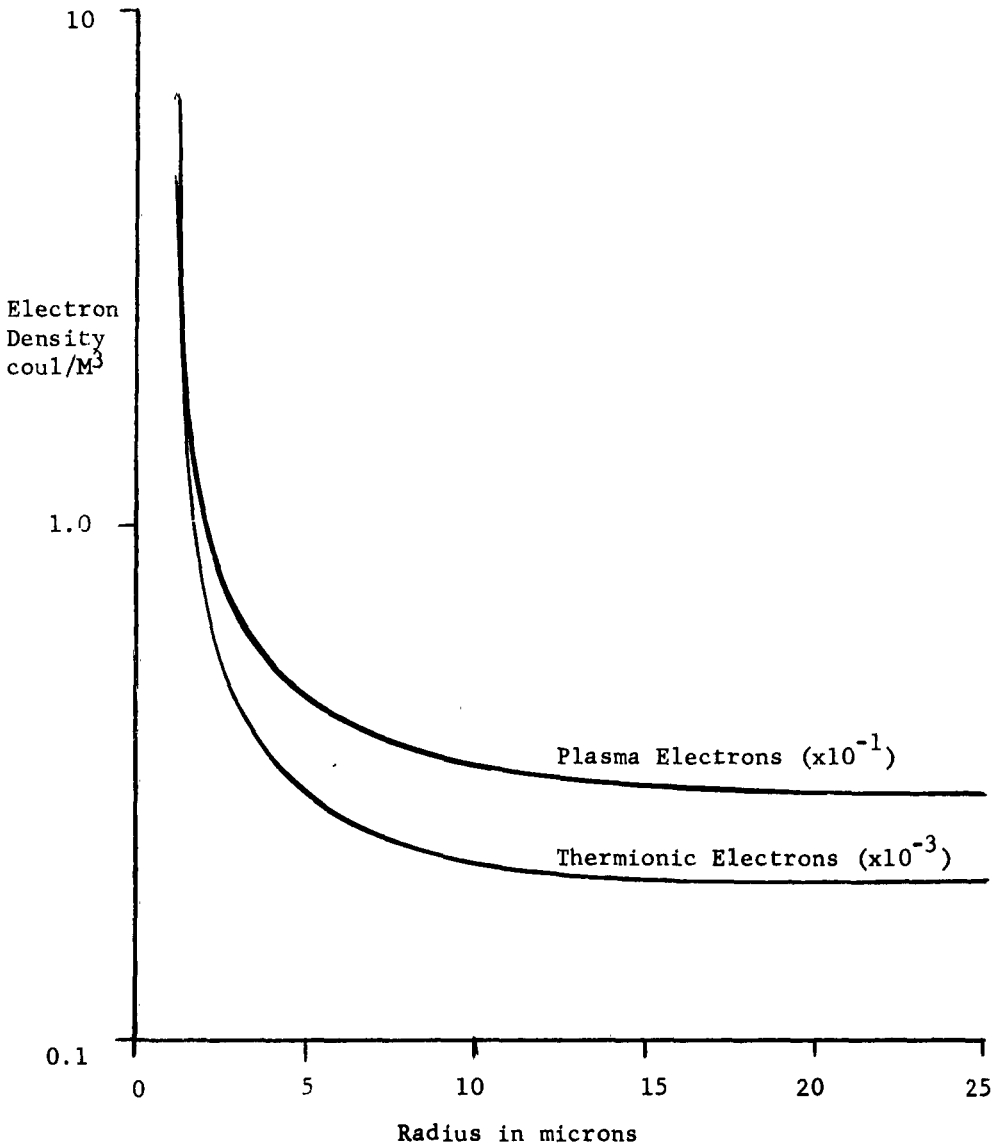

Fig. 12. The electron concentration near and aluminum oxide particle is shown where the effect of plasma ions and electrons is taken into account. Electrons from thermionic emission and from ionization in the plasma are shown separately.

Analytical solutions are available over limited regions of the curve. The Debye-Hückel theory is good over a certain range of larger r values. Near the minimum point in ρ the voltage is given by

$$V = \frac{e\rho_\epsilon r_p^2}{6\epsilon_o} \left[\left(\frac{r}{r_p}\right)^2 + 2 \left(\frac{r_p}{r}\right) - 3 \right] \qquad (15)$$

where r_p = radius at V = 0, the plasma voltage, and ρ_ϵ is the plasma density due to thermionic emission. An accurate analytical solution is also available near the particle surface. Solutions in this region are obtained by neglecting the space charge contribution.

DISTRIBUTION LIST

NO. OF COPIES	AGENCY	NO. OF COPIES	AGENCY
2	Asst. Sec. of Defense for Research and Development Information Office Library Branch Pentagon Building Washington 25, D. C.	10	Armed Services Technical Information Agency Documents Service Center Arlington Hall Station Arlington 12, Virginia
6	Director, Naval Research Laboratory Technical Information Officer (Code 2000) Washington 25, D. C.	2	Chief of Naval Research Electronics Branch (Code 427) Department of the Navy Washington 25, D. C.
1	Electronics Research Directorate Library Air Force Cambridge Research Center Laurence G. Hanscom Field Bedford, Massachusetts	1	Commanding Officer ONR Branch Office The John Crerar Library Building 86 E. Randolph Street Chicago 1, Illinois
1	Commanding Officer ONR Branch Office 1030 East Green Street Pasadena 1, California	1	Commanding Officer ONR Branch Office 346 Broadway New York 13, New York
2	Commanding Officer Office of Naval Research Navy No. 100, Fleet Post Office New York, New York (Box 39)	1	Office of Technical Services Technical Reports Sections Department of Commerce Washington 25, D. C.
1	Commander Air Force Office of Scientific Research Washington 25, D. C. ATTN: SRY	1	Office of Ordnance Research Box CM, Duke Station Durham, North Carolina
1	Director, Naval Research Laboratory (Code 6430) Washington 25, D. C.	2	Chief, Bureau of Ships (Code 816c) Department of the Navy Washington 25, D. C.
1	ASRNEA Wright-Patterson Air Force Base Ohio	1	Librarian U.S. Naval Ordnance Laboratory White Oak, Maryland

NO. OF COPIES	AGENCY
1	Director, Naval Research Laboratory (Code 5200) Washington 25, D. C.
1	Commanding Officer U. S. Army Electronics Reaearch and Development Laboratory Fort Monmouth, New Jersey Attention: Institute for Exploratory Research
1	Chief, Bureau of Ships (Code 327) Department of the Navy Washington 25, D. C.
1	Chief, Bureau of Aeronautics (Code EL-412.1) Department of the Navy Washington 25, D. C.
2	Librarian, National Bureau of Standards Department of Commerce Washington 25, D. C.
1	Advisory Group on Electron Tubes Secretary, Working Group on Semiconductor Devices 346 Broadway New York 13, New York
1	Commanding Officer Wright Air Development Center Wright-Patterson Air Force Base Ohio
1	Research Laboratory for Electronics Massachusetts Institute of Technology Cambridge, Massachusetts

NO.OF COPIES	AGENCY
1	Director National Science Foundation Washington 25, D. C.
1	Commanding Officer Office of Naval Research Branch Office 1000 Geary Street San Francisco 9, California
1	Director U. S. Naval Electronics Laboratory San Diego 52, California
1	Applied Physics Laboratory Johns Hopkins University Silver Spring, Maryland
1	Chief, Bureau of Ordnance (Code RE P) Department of the Navy Washington 25, D. C.
1	Solid State Group Hughes Aircraft Company Research and Development Laboratories Culver City, California
1	Solid State Development Branch Evans Signal Laboratories Belmar, New Jersey
1	Chief, Bureau of Ordnance (Code RE 9) Department of the Navy Washington 25, C. C.

NO. OF COPIES	AGENCY	NO. OF COPIES	AGENCY
1	Navy Representative, Project Lincoln Massachusetts Institute of Technology Building B, Lincoln Laboratory P. O. Box 73 Lexington 73, Massachusetts	1	Chief, BuShips ATTN: Code 681A1D Dept of Navy Washington 25, D. C.
1	Commanding Officer U. S. Army Signal Research and Development Laboratories Fort Monmouth, New Jersey ATTN: SIGRA/SL-PFA	1	USASRDL (SIGRA/SL-PRT) Ft. Monmouth, New Jersey
1	Library U. S. Naval Ordnance Plant Indianapolis, Indiana	1	AFCRL (CRRCPV) ATTN: Electronic Material Sciences Laboratory L. G. Hanscom Field Bedford, Massachusetts
4	Advisory Group on Electron Devices ATTN: H. N. Serig 346 Broadway, 8th Floor New York 13, New York	1	RADC (RCCIL-2) ATTN: Documents Library Griffiss AFB, New York
1	Scientific and Technical Information Facility ATTN: NASA Representative (S-AK/DL) P. O. Box 5700 Bethesda, Maryland	2	ASD (ASRNET-3) Wright-Patterson AFB, Ohio